© 2021. Published by The Company of Biologists Ltd | Journal of Cell Science (2022) 135, jcs258186. doi:10.1242/jcs.258186

RESEARCH ARTICLE

SPECIAL ISSUE: CELL BIOLOGY OF LIPIDS

Ca^{2+}-dependent protein acyltransferase DHHC21 controls activation of $CD4^+$ T cells

Shayahati Bieerkehazhi*,[1], Ying Fan*,[1,2], Savannah J. West[1,3], Ritika Tewari[1], Junsuk Ko[1,3], Tingting Mills[1], Darren Boehning[2] and Askar M. Akimzhanov[1,‡]

ABSTRACT

Despite the recognized significance of reversible protein lipidation (S-acylation) for T cell receptor signal transduction, the enzymatic control of this post-translational modification in T cells remains poorly understood. Here, we demonstrate that DHHC21 (also known as ZDHHC21), a member of the DHHC family of mammalian protein acyltransferases, mediates T cell receptor-induced S-acylation of proximal T cell signaling proteins. Using $Zdhhc21^{dep}$ mice, which express a functionally deficient version of DHHC21, we show that DHHC21 is a Ca^{2+}/calmodulin-dependent enzyme critical for activation of naïve $CD4^+$ T cells in response to T cell receptor stimulation. We find that disruption of the Ca^{2+}/calmodulin-binding domain of DHHC21 does not affect thymic T cell development but prevents differentiation of peripheral $CD4^+$ T cells into Th1, Th2 and Th17 effector T helper lineages. Our findings identify DHHC21 as an essential component of the T cell receptor signaling machinery and define a new role for protein acyltransferases in regulation of T cell-mediated immunity.

KEY WORDS: Palmitoylation, S-acylation, T cell receptor, Protein acyltransferase, Calmodulin

INTRODUCTION

$CD4^+$ T cells are the master regulators of the adaptive immune response. During pathogen invasion, naïve $CD4^+$ T cells become activated and differentiate into effector T helper (Th) lineages (Zhou et al., 2009). Activation of $CD4^+$ T cells is initiated upon engagement of the T cell receptor (TCR) by the antigen–major histocompatibility complex on the surface of the antigen-presenting cell (Brownlie and Zamoyska, 2013; Salmond et al., 2009). Ligation of the TCR by a foreign antigen triggers activation of Src-family kinases Lck and Fyn leading to phosphorylation of the TCR-associated CD3ζ chain (Palacios and Weiss, 2004; Salmond et al., 2009). Phosphorylated TCR–CD3 complex amplifies the initial antigenic signal through recruitment of another regulatory kinase, ZAP-70 (Katz et al., 2017). Activated ZAP-70 proceeds to phosphorylate its downstream targets, primarily membrane-bound scaffolding proteins LAT and SLP-76 (also known as LCP2) (Au-Yeung et al., 2018). Phosphorylated LAT and SLP-76 nucleate assembly of the multiprotein signaling complex termed the 'signalosome'. Formation of the signalosome further propagates the TCR signaling pathway resulting in activation of the important downstream mediators, such as phospholipase C-γ1 (PLC-γ1) and cytoplasmic Ca^{2+} influx, and, ultimately, leads to the transcriptional responses associated with activation and clonal expansion of $CD4^+$ T cells (Katz et al., 2017; Smith-Garvin et al., 2009; Stathopulos et al., 2008; Su et al., 2016).

A number of proteins critically involved in regulation of the TCR signaling pathway have been found to be S-acylated. Protein S-acylation (also known as S-palmitoylation) is a post-translational modification of cysteine thiols with long-chain fatty acids (Resh, 2016). Kinases Lck and Fyn were among the first mammalian proteins identified as being S-acylated and this modification has been demonstrated to be necessary for their signaling function in T cells (Kabouridis et al., 1997; Koegl et al., 1994; van't Hof and Resh, 1999; Wolven et al., 1997). The transmembrane adaptor LAT has been reported to be dually S-acylated at cysteine residues located proximally to the inner face of the plasma membrane, and a selective defect in LAT S-acylation has been found to be associated with a state of T cell functional unresponsiveness known as T cell anergy (Hundt et al., 2006). Recently, a candidate-based screening of the proximal TCR signaling components allowed us to detect previously uncharacterized S-acylation of adaptor protein GRB2, PLC-γ1 and tyrosine kinase ZAP-70 (Fan et al., 2020; Tewari et al., 2021). A functional analysis of ZAP-70 S-acylation revealed that this modification is essential for ZAP-70 interaction with its protein substrates and subsequent transcriptional responses (Tewari et al., 2021). Thus, S-acylation of T cell signaling proteins is emerging as an important regulatory mechanism controlling T cell activation and function. However, the enzymatic control of protein S-acylation in T cells remains enigmatic.

S-acylation of the mammalian proteins is catalyzed by a family of 23 protein acyltransferases with a common DHHC (Asp-His-His-Cys) motif within the catalytic core and, typically, four transmembrane domains (Baekkeskov and Kanaani, 2009). In our previous studies, we identified a member of this family, DHHC21 (also known as ZDHHC21), as a protein acyltransferase mediating S-acylation of several proximal T cell signaling proteins (Fan et al., 2020). Downregulation of DHHC21 in EL4 mouse lymphoma cells resulted in their unresponsiveness to TCR stimulation, suggesting that DHHC21 can be a critical regulator of the T cell effector function (Fan et al., 2020). To evaluate the contribution of DHHC21 to T cell-mediated immunity in an animal model, we used $Zdhhc21^{dep}$ mice, which express a functionally deficient DHHC21 carrying an in-frame mutation resulting in a loss of a phenylalanine in position 233 (ΔF233) (Mayer et al., 1976; Mill et al., 2009). We found that deletion of F233 disrupts TCR-induced calmodulin binding to DHHC21

[1]Department of Biochemistry and Molecular Biology, McGovern Medical School, University of Texas Health Science Center at Houston, Houston, TX 77030, USA. [2]Cooper Medical School of Rowan University, Camden, NJ 08103, USA. [3]MD Anderson Cancer Center and University of Texas Health Science at Houston Graduate School, Houston, TX 77030, USA.
*These authors contributed equally to this work

‡Author for correspondence (Askar.M.Akimzhanov@uth.tmc.edu)

S.B., 0000-0001-9520-4118; D.B., 0000-0001-7920-6922; A.M.A., 0000-0002-5592-8215

Handling Editor: James Olzmann
Received 10 December 2020; Accepted 13 April 2021

Journal of Cell Science (2022) 135, jcs258186. doi:10.1242/jcs.258186

indicating that DHHC21 is a Ca^{2+}-regulated enzyme. Using the acyl-resin assisted capture (Acyl-RAC) technique, we found that the ΔF233 mutant of DHHC21 was unable to mediate TCR-induced S-acylation of critical T cell signaling proteins, resulting in diminished activation of the TCR pathway. Although expression of the ΔF233 mutant did not affect T cell development, naïve $CD4^+$ cells isolated from peripheral lymphoid organs of $Zdhhc21^{dep}$ mice exhibited decreased activation of the proximal TCR signaling components and suppressed cytoplasmic Ca^{2+} release in response to TCR stimulation. Consequently, $Zdhhc21^{dep}$ $CD4^+$ T cells showed significantly decreased upregulation of the surface activation marker CD69 and reduced production of the pro-inflammatory cytokine interleukin-2 (IL-2) upon extended stimulation of the TCR. Furthermore, the impaired DHHC21 function prevented naïve $Zdhhc21^{dep}$ $CD4^+$ T cells from differentiating into effector T helper subtypes, suggesting that protein acyltransferase DHHC21 plays an important role in peripheral T cell immunity.

RESULTS

F233 is required for Ca^{2+}-dependent calmodulin binding to DHHC21

The spontaneous depilated (‘dep’) mutation of DHHC21 ($Zdhhc21^{dep}$, MGI:94884) was initially described as a recessive mutation on chromosome 4 characterized by variable hair loss and abnormal hair structure and was later mapped to the *Zdhhc21* gene, where a deletion of F233 was found (Mayer et al., 1976; Mill et al., 2009). The delayed follicle differentiation, endothelial dysfunction and reduced vascular tone observed in $Zdhhc21^{dep}$ mice (Beard et al., 2016; Marin et al., 2016; Mill et al., 2009) suggested that deletion of F233 causes a functional deficiency of DHHC21. However, the molecular mechanism underlying dysfunction of the ΔF233 DHHC21 mutant remained unresolved.

Our analysis of the primary DHHC21 sequence revealed that F233 is located within a putative 1-14 Ca^{2+}/calmodulin-binding motif at the C-terminal cytoplasmic tail of the enzyme (Fig. 1A). To experimentally validate calmodulin binding to DHHC21, we performed a co-immunoprecipitation assay using $CD4^+$ T cells isolated from wild-type (WT) and $Zdhhc21^{dep}$ mice. To determine whether DHHC21 interacts with calmodulin in a Ca^{2+}-dependent manner, we treated cells with thapsigargin (TG), a potent SERCA pump inhibitor (Michelangeli and East, 2011), to invoke a cytoplasmic Ca^{2+} influx from the endoplasmic reticulum (ER) stores. Endogenously expressed DHHC21 was then immunoprecipitated from the cell lysates and analyzed by immunoblotting. As shown in Fig. 1B, treatment of WT $CD4^+$ T cells with 10 µM TG resulted in co-immunoprecipitation of DHHC21 with calmodulin indicating the presence of a functional Ca^{2+}/calmodulin-binding domain. However, calmodulin was not detected in DHHC21 immunoprecipitates from $Zdhhc21^{dep}$ $CD4^+$ T cells suggesting that deletion of F233 disrupts binding between

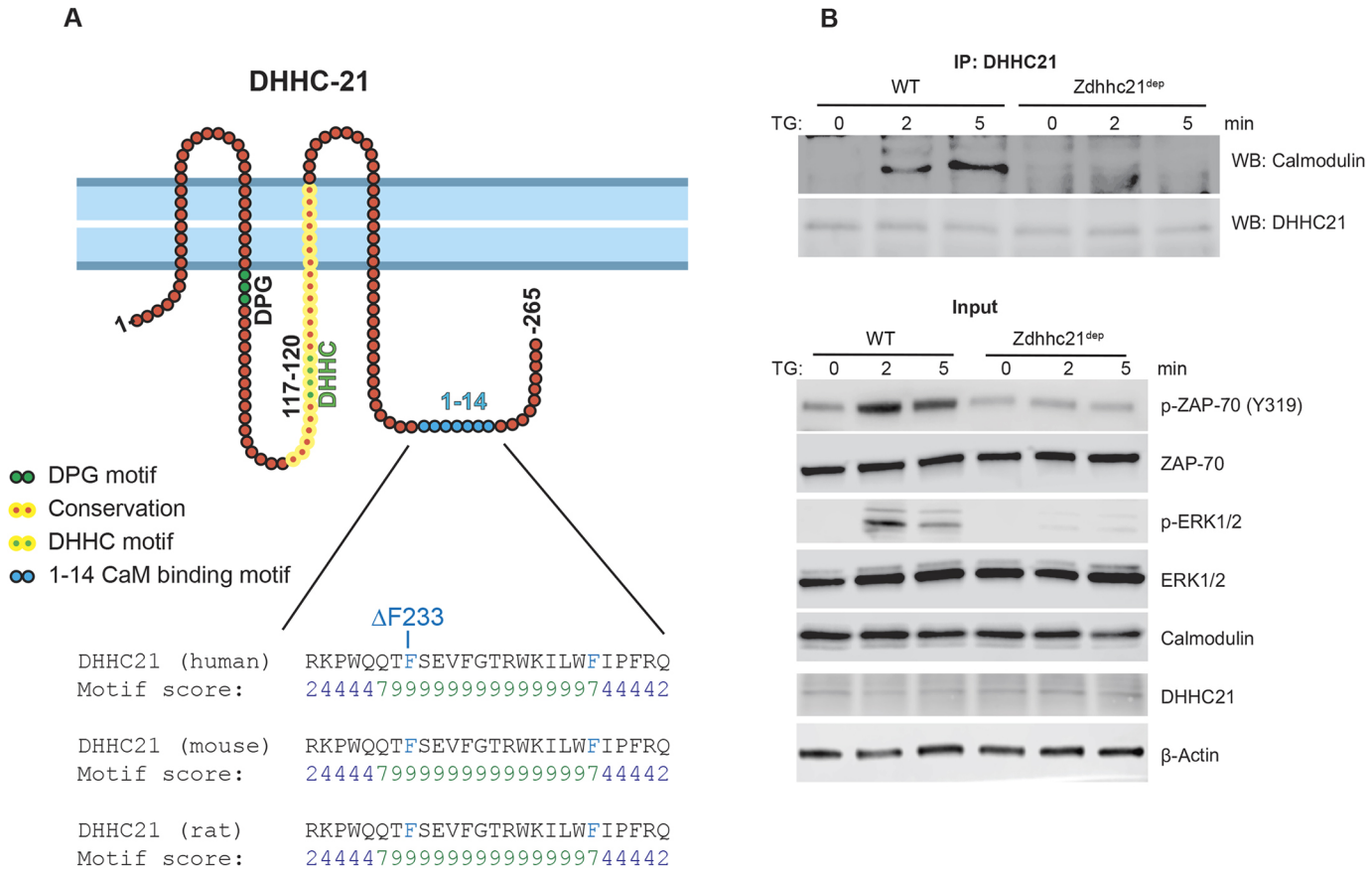

Fig. 1. DHHC21 has a Ca^{2+}/calmodulin-binding motif. (A) Schematic depiction of DHHC21 illustrating the approximate localization of the predicted 1-14 Ca^{2+}/calmodulin-binding motif within the C-terminal cytoplasmic tail. The 1-14 motif is completely conserved between species. Location of the ‘dep’ mutation (ΔF233) is indicated. (B) Ca^{2+}-dependent co-immunoprecipitation of DHHC21 and calmodulin. $CD4^+$ T cells from WT or $Zdhhc^{dep}$ mice were treated for the indicated times with 10 µM thapsigargin (TG) to evoke Ca^{2+} release. DHHC21 was immunoprecipitated from the cell lysates and binding of calmodulin was detected by immunoblotting. Total lysates (20% of load) are depicted as input. Phosphorylated ZAP-70 and ERK1/2 are shown to confirm $CD4^+$ T cells’ responses to TCR-stimulation. Blots are representative of three repeats.

Journal of Cell Science (2022) 135, jcs258186. doi:10.1242/jcs.258186

DHHC21 and calmodulin (Fig. 1B). Similarly, stimulation of $CD4^+$ T cells with cross-linked anti-CD3–CD28 antibodies resulted in calmodulin binding to WT DHHC21 but not to the ΔF233 mutant (Fig. S1). Since calmodulin is known to relay Ca^{2+} signals through direct binding to its targets, these observations suggest that the ΔF233 mutation could prevent activation of the enzyme in response to TCR-induced Ca^{2+} release, thus leading to functional deficiency of DHHC21.

DHHC21 mediates TCR-induced S-acylation of T cell signaling proteins

We next sought to examine the effect of the ΔF233 mutation on the acyltransferase activity of DHHC21. Previously, we detected direct stimulus-dependent interaction between DHHC21 and the Src-family kinase Lck (Fan et al., 2020). Furthermore, we showed that shRNA-mediated downregulation of DHHC21 significantly decreased S-acylation of Lck and PLC-γ1 in resting EL4 lymphoma cells, suggesting that these proteins are direct targets of DHHC21 (Fan et al., 2020). To test whether ΔF233 DHHC21 is able to mediate S-acylation of its protein substrates, we isolated $CD4^+$ T cells from spleen and lymph nodes of WT and $Zdhhc21^{dep}$ mice and subjected them to the acyl-resin assisted capture (Acyl-RAC) assay (Fig. 2A) (Tewari et al., 2020). Briefly, in this assay, free thiol groups in cell lysates are blocked with S-methyl methanethiosulfonate (MMTS) and the thioester bond between cysteine residues and fatty acid moieties is selectively cleaved with neutral hydroxylamine (HA). The newly exposed cysteine thiol groups are then reacted with a thiol-reactive resin to capture the S-acylated proteins. As shown in Fig. 2B, C, deletion of F233 did not affect basal S-acylation levels of Lck, PLC-γ1 and ERK1 and ERK2 (ERK1/2; also known as MAPK3 and MAPK1, respectively) proteins in quiescent T cells. In WT $CD4^+$ T cells, short-term TCR stimulation with cross-linked anti-CD3–CD28 antibodies resulted in increased S-acylation of Lck, ERK1/2 and PLC-γ1. However, we did not observe TCR-induced S-acylation of these proteins in $CD4^+$ T cells isolated from $Zdhhc21^{dep}$ mice (Fig. 2). Our observations suggest that although ΔF233 DHHC21 can still support basal lipidation, a functional Ca^{2+}/calmodulin-binding domain is required to mediate antigen-induced S-acylation of DHHC21 protein substrates. These results were also consistent with previously reported substrate specificity of DHHC21 toward Lck and PLC-γ1 (Fan et al., 2020), and indicate that ERK1/2, recently identified as a novel S-acylated protein in T cells (data not shown), could be another target of DHHC21.

DHHC21 is required for initiation of the TCR signaling pathway

Our data indicate that loss of F233 inhibits the ability of DHHC21 to S-acylate its targets in response to TCR stimulation. Since identified DHHC21 protein substrates are components of the proximal TCR pathway, we next aimed to determine whether the functional deficiency of ΔF233 DHHC21 affects initiation of the early TCR signaling events. $CD4^+$ T cells purified from spleen and lymph nodes of WT and $Zdhhc21^{dep}$ mice were stimulated with cross-linked anti-CD3–CD28 antibodies and phosphorylation of key TCR signaling proteins was analyzed by immunoblotting. We found that activation of the first signaling TCR kinase Lck, as measured through phospho-Src family antibody, was diminished in $Zdhhc21^{dep}$ $CD4^+$ T cells (Fig. 3A,B). TCR-induced activation of the critical downstream proteins ZAP-70, LAT, PLC-γ1, ERK1/2, and the JNK and p38 family proteins was also suppressed in these cells indicating that DHHC21 could be one of the earliest signal mediators in the TCR pathway.

Ca^{2+} serves as a critical second messenger during T cell activation. The cytoplasmic Ca^{2+} influx is triggered upon TCR-dependent activation of PLC-γ1, which generates the inositol-1,4,5-trisphosphate required for rapid Ca^{2+} release from the ER stores (Lewis, 2001; Oh-hora, 2009). To further test the role of DHHC21 in initiation of the proximal TCR signaling cascade, we loaded WT and $Zdhhc21^{dep}$ $CD4^+$ T cells with the Fura-2 Ca^{2+} indicator and assessed changes in cytoplasmic Ca^{2+} concentration upon T cell activation. Stimulation of the TCR with anti-CD3–CD28 antibodies evoked immediate Ca^{2+} responses in ∼80% of the WT $CD4^+$ T cells (Fig. 3C–E). Consistent with inhibited activation of PLC-γ1, we found that TCR engagement induced Ca^{2+} release in only ∼20% of $Zdhhc21^{dep}$ $CD4^+$ T cells and the cytoplasmic Ca^{2+} concentrations peaked at significantly reduced levels (Fig. 3C–E). This result indicates that fully functional DHHC21 is required to support normal Ca^{2+} dynamics in stimulated T cells.

Suppressed T cell activation in $Zdhhc21^{dep}$ mice

Thus far, our results show that the ΔF233 mutation of DHHC21 causes disruption of the early TCR signaling events, including activation of regulatory kinases and Ca^{2+} mobilization from the ER. To further investigate the role of DHHC21 in T cell activation, we stimulated $CD4^+$ T cells isolated from $Zdhhc21^{dep}$ mice and their WT littermates with plate-bound anti-CD3–CD28 antibodies for 24 h and assessed induction of T cell activation markers. We found that in contrast to WT cells, activated $Zdhhc21^{dep}$ $CD4^+$ T cells showed markedly decreased surface expression of CD69 (Fig. 4A,B). Similarly, production of the pro-inflammatory cytokine IL-2 in response to TCR stimulation was significantly reduced in $CD4^+$T cells expressing the ΔF233 DHHC21 mutant (Fig. 4C). Thus, consistent with previous observations, our data suggest that DHHC21 is required for T cell activation upon TCR engagement.

F233 is dispensable for T cell development

To examine a possible role of DHHC21 in T cell development and differentiation, we assessed the frequency of major T cell subpopulations in 4–6-week-old $Zdhhc21^{dep}$ mice and their WT littermates in thymus and peripheral lymphoid organs. Flow cytometry analysis of double-negative (DN; $CD4^-CD8^-$), double-positive (DP; $CD4^+CD8^+$) and single positive (SP; $CD4^+CD8^-$ and $CD4^-CD8^+$) thymocytes revealed no difference in relative proportions of these populations (Fig. 5A). The total numbers of thymocytes and thymus size were also similar in WT and $Zdhhc21^{dep}$ mice and no difference was detected in expression of CD44 and CD25 on the surface of the DN thymocytes (data not shown and Fig. 5A,B) suggesting that the ΔF233 DHHC21 mutation did not affect DN-to-DP and DP-to-SP transitions during T cell maturation. Similarly, the functional deficiency of DHHC21 did not perturb development of regulatory (Treg) cells in thymus of $Zdhhc21^{dep}$ mice (Fig. 5C).

The analysis of T cell populations in peripheral lymphoid organs also showed no substantial differences between $CD4^+$ and $CD8^+$ T cell percentages in WT and $Zdhhc21^{dep}$ mice (Fig. 6A). Similarly, no changes were detected in populations of naïve ($CD44^{lo}CD62L^{hi}$), effector memory ($CD44^{hi}CD62L^{lo}$), and Treg T cells (Fig. 6B,C). However, we noted the consistent increase in size of spleen and lymph nodes of $Zdhhc21^{dep}$ mice accompanied by statistically significant increases in absolute cell numbers (Fig. 6D,E), indicating that the attenuated DHHC21 function could affect regulation of the peripheral T cell immunity.

Journal of Cell Science (2022) 135, jcs258186. doi:10.1242/jcs.258186

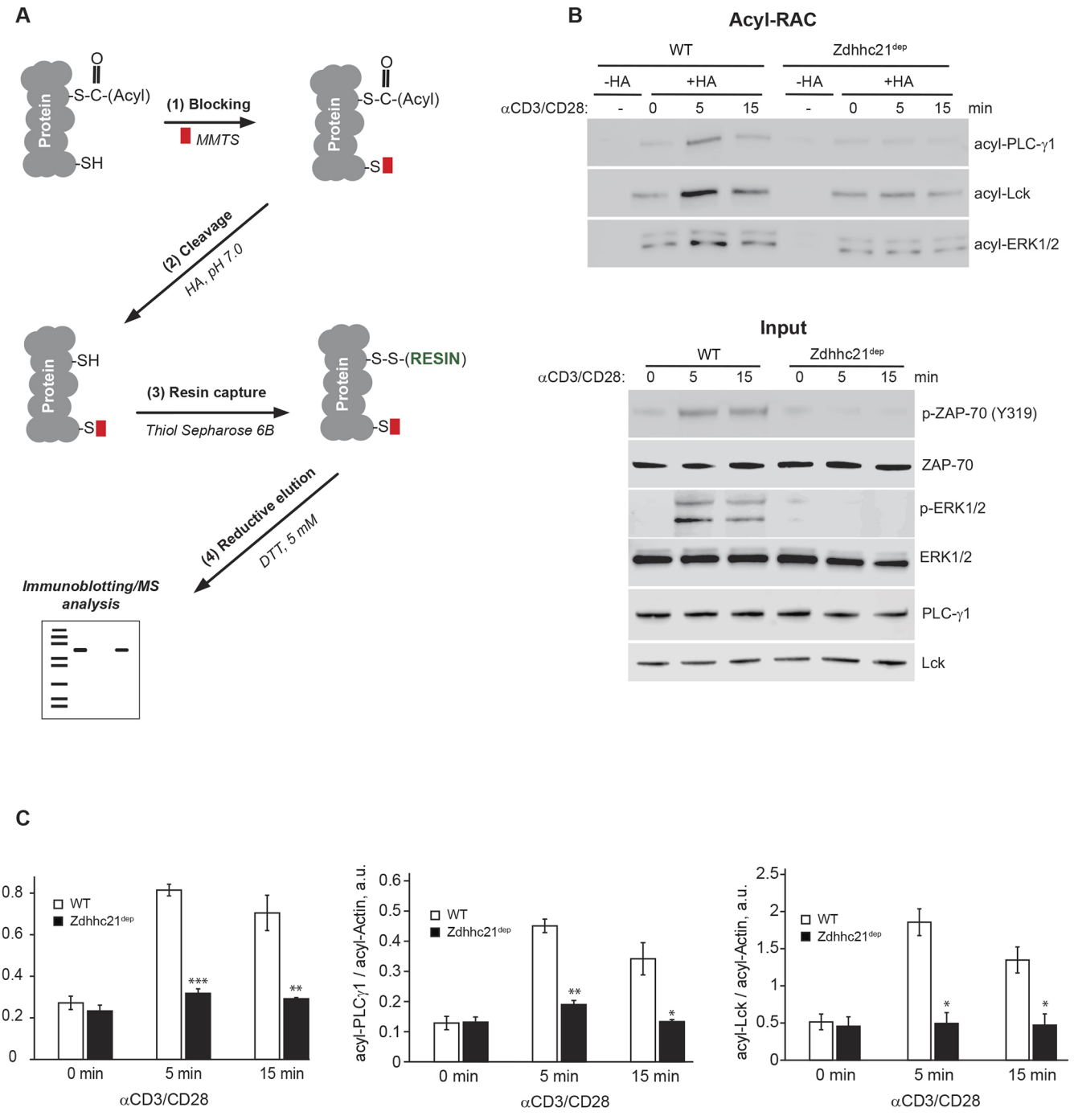

Fig. 2. DHHC21 mediates TCR-induced S-acylation of signaling proteins. (A) Overview of the acyl-resin assisted capture (Acyl-RAC) assay. Free cysteine thiols (-SH) are irreversibly blocked by S-methyl methanethiosulfonate (MMTS) following cell lysis. Thioester bonds between cysteine resdiues and acyl groups are then specifically cleaved by neutral hydroxylamine (HA). The newly formed free thiol groups are captured by the thiol-reactive Sepharose and S-acylated proteins are detected by immunoblotting. (B) TCR-induced protein S-acylation. $CD4^+$ T cells from WT or $Zdhhc21^{dep}$ mice were stimulated with cross-linked anti-CD3–CD28 antibodies for the indicated times, and protein S-acylation (acyl-) was determined using the Acyl-RAC assay. Samples not treated with hydroxylamine (-HA) were used as a negative control. β-actin, a known S-acylated protein (Ren et al., 2013), was used as a loading control. Total lysates prior to addition of HA (5% of load) are depicted as input. Phosphorylated ZAP-70 and ERK1/2 are shown to confirm cellular responses to TG-induced changes in cytoplasmic Ca^{2+} levels. (C) Quantitative analysis of protein S-acylation in response to TCR stimulation with cross-linked anti-CD3–CD28 (αCD3/CD28) antibodies. Error bars represent mean±s.e.m., n=3. *P<0.05; **P<0.01; ***P<0.001 (two-tailed, unpaired Student's t-test). a.u., arbitrary units.

DHHC21 is important for peripheral $CD4^+$ T cell immunity

Given the critical role of DHHC21 in TCR-mediated T cell activation, we hypothesized that expression of the functionally deficient ΔF233 DHHC21 mutant affects the ability of naïve $CD4^+$ T cells to differentiate into functionally distinct effector T helper (Th) cell lineages. To test this hypothesis, we isolated naïve $CD4^+$ T cells from spleen and lymph nodes of WT and $Zdhhc21^{dep}$ mice and incubated them under Th1, Th2, or Th17 polarizing conditions. After 5 days, cells were re-stimulated with plate-bound anti-CD3–CD28 antibodies and production of lineage specific cytokines was

Journal of Cell Science (2022) 135, jcs258186. doi:10.1242/jcs.258186

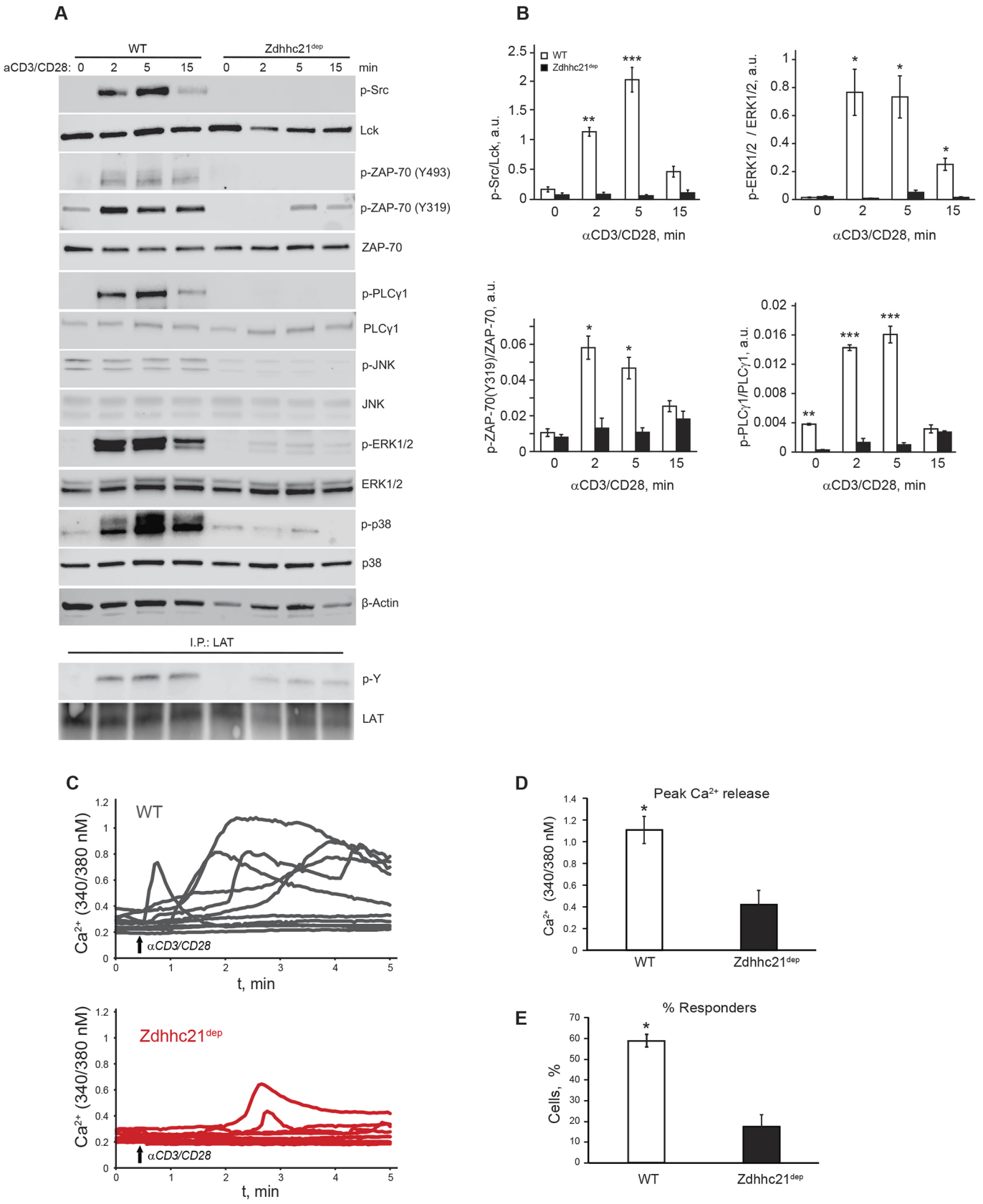

Fig. 3. See next page for legend.

Journal of Cell Science (2022) 135, jcs258186. doi:10.1242/jcs.258186

Fig. 3. TCR signaling is impaired in Zdhhc21^{dep} CD4^{+} T cells. (A) CD4^{+}T cells from WT or Zdhhc21^{dep} mice were stimulated with cross-linked anti-CD3–CD28 (aCD3/CD28) antibodies for indicated times and indicated phospho-proteins (p-) and total proteins were analyzed by immunoblotting. β-actin was used as a loading control. The results shown are representative of three independent experiments. (B) Quantitative analysis of phosphorylation of TCR signaling proteins in response to TCR stimulation with cross-linked anti-CD3–CD28 antibodies. Error bars represent mean±s.e.m., *n*=3. **P*<0.05; ***P*<0.01; ****P*<0.001 (two-tailed, unpaired Student's *t*-test). a.u., arbitrary units. (C) CD4^{+} T cells were loaded with Fura-2 Ca^{2+} indicator and pre-incubated with anti-CD3–CD28 antibodies. IgG antibody was added to induce cross-linking after an observation period (upward arrow). Shown are representative traces from single WT (gray) and Zdhhc21^{dep} (red) cells. (D) Peak Ca^{2+} release. CD4^{+} T cells were treated as described in B. Data represent maximum Ca^{2+} values averaged from four independent experiments (~100 WT or Zdhhc21^{dep} cells per experiment). Data represent mean±s.e.m. **P*<0.05 (two-tailed, unpaired Student's *t*-test). (E) Ca^{2+} response pattern. CD4^{+}T cells were treated as described in B. Cells showing at least a 10% increase in Ca^{2+} values upon TCR stimulation were identified as responders. Data represent mean±s.e.m. percentage of responders from four independent experiments (~100 WT or Zdhhc21^{dep} CD4^{+}T cells per experiment). **P*<0.05 (two-tailed, unpaired Student's *t*-test).

assessed with ELISA. As shown in Fig. 7A, Zdhhc21^{dep} CD4^{+} T cells produced significantly less IFN-γ cytokine when cultured under Th1 conditions. Under Th2 polarizing conditions, Zdhhc21^{dep} CD4^{+} T cells failed to secrete IL-6 and IL-13 cytokines. Under Th17 conditions, we observed significantly decreased production of IL-17A in Zdhhc21^{dep} CD4^{+} T cells when compared to WT CD4^{+} T cells. Interestingly, IFN-γ production under Th17 conditions was increased in Zdhhc21^{dep} CD4^{+} T cells indicating a possible role of DHHC21 in Th17-mediated autoimmunity.

To further examine the role of DHHC21 in effector T cell differentiation, we used real-time PCR to assess expression of lineage-specific transcription factors in CD4^{+} T cells polarized under Th1, Th2 or Th17 conditions. We found that in comparison to WT cells, CD4^{+} T cells from Zdhhc21^{dep} mice demonstrated significantly decreased expression of T-bet (*Tbx21*) under Th1 and Th17 conditions, and failed to upregulate expression of GATA-3 under Th2 conditions (Fig. 7B). Likewise, upregulation of RORγτ and RORα (*Rorc* and *Rora*), the signature Th17 genes, was significantly diminished in Zdhhc21^{dep} CD4^{+} T cells differentiated under Th17 conditions (Fig. 7B). Overall, our data indicate that DHHC21 is not only important for initial T cell activation but also required for proper differentiation of peripheral CD4^{+} T cells into major T helper lineages.

DISCUSSION

Several classes of regulatory enzymes cooperate to ensure proper activation of T cells in response to invading pathogens. Here, we report a previously uncharacterized role of protein acyltransferases – enzymes mediating reversible protein S-acylation – in regulation of T cell function. Specifically, our study demonstrates that DHHC21, a member of the DHHC family of mammalian protein acyltransferases, is essential for TCR-dependent CD4^{+} T cell activation and subsequent differentiation into major T helper lineages.

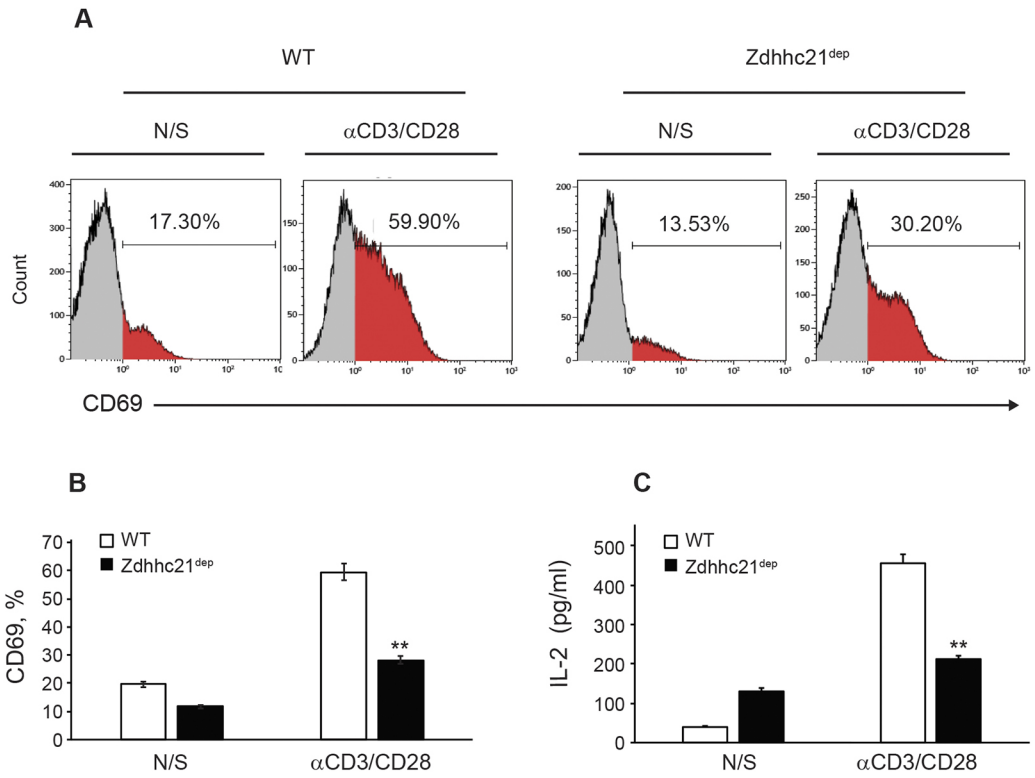

Fig. 4. DHHC21 is required for T cell activation. (A) Surface expression of CD69 on CD4^{+} T cells from WT or Zdhhc21^{dep} mice. CD4^{+} T cells were stimulated or not (N/S) with plate-bound anti-CD3–CD28 antibodies (αCD3/CD28) for 24 h and analyzed by flow cytometry. The red section indicates the population of CD69^{+} cells (given as a percentage). (B) Average a percentage of CD69^{+} T cells from WT or Zdhhc21^{dep} mice. CD4^{+} T cells were stimulated with plate-bound anti-CD3–CD28 antibodies for 24 h and analyzed by flow cytometry. The graph shows mean±s.d. from three independent experiments. ***P*<0.01 (two-tailed, unpaired Student's *t*-test). (C) IL-2 production by CD4^{+} T cells from WT or Zdhhc21^{dep} mice. CD4^{+} T cells were stimulated with plate-bound anti-CD3/CD28 antibodies for 24 h and collected supernatants were assayed by ELISA. The graph shows mean±s.d. values, *n*=3, ***P*<0.01 (two-tailed, unpaired Student's *t*-test).

Journal of Cell Science (2022) 135, jcs258186. doi:10.1242/jcs.258186

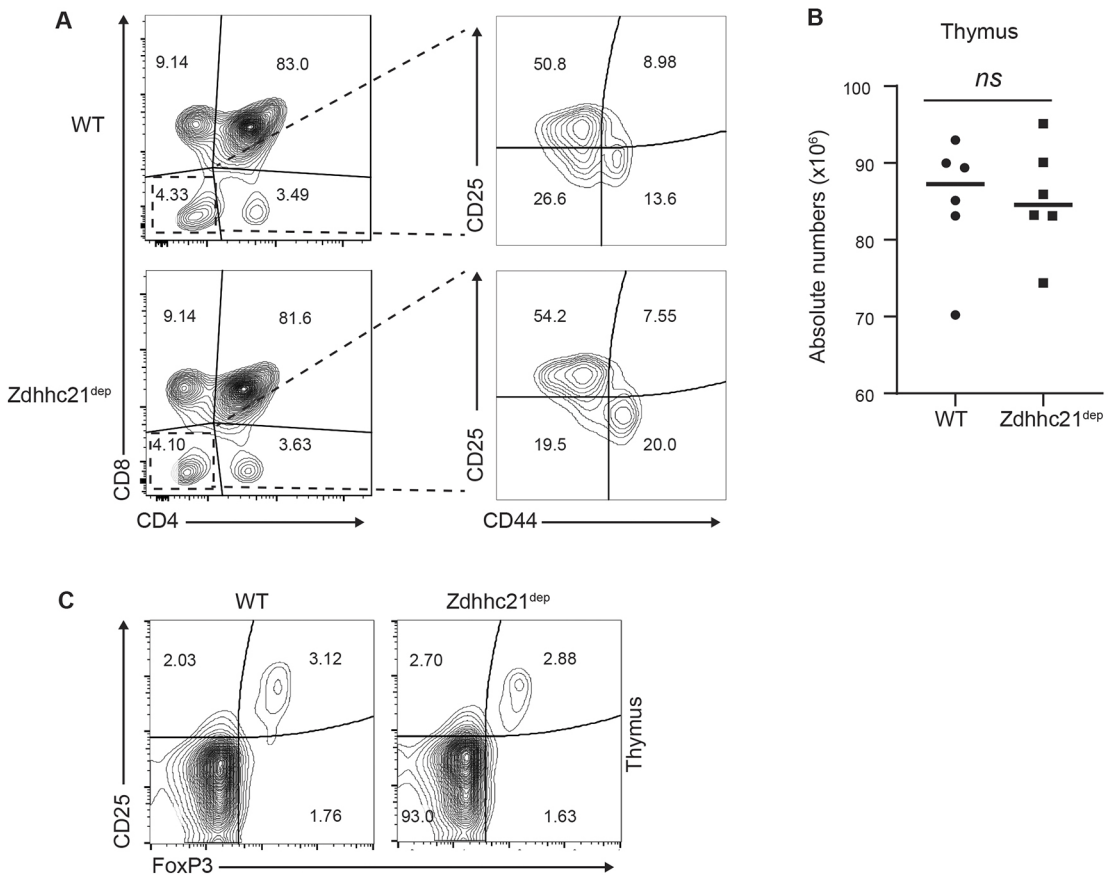

Fig. 5. Thymocyte development in Zdhhc21^{dep} mice. (A) Flow cytometry analysis of cells isolated from thymus of WT and Zdhhc21^{dep} mice. Plots of CD4$^+$ and CD8$^+$ cells are gated on CD3$^+$ cells. Plots of CD25$^+$ and CD44$^+$ cells are gated on CD4$^-$CD8$^-$ cells. Values are percentages for each section. (B) The absolute numbers of thymocytes from WT and Zdhhc21^{dep} mice. Cell numbers were calculated based on the relative percentages determined by flow cytometry analysis and total cell numbers from thymus. ns, not significant, P>0.05 (two-tailed, unpaired Student's t-test). (C) Flow cytometry analysis of Treg cells isolated from thymus of WT and Zdhhc21^{dep} mice. Plots of CD25$^+$ and FoxP3$^+$ cells are gated on CD4$^+$ cells. Values are percentages for each section.

The importance of protein S-acylation for the T cell immune responses has become evident since the discovery that this post-translational modification critically affects the plasma membrane localization and function of well-characterized components of the canonical TCR signaling pathway, such as Lck, Fyn, LAT and, recently, ZAP-70 (Hundt et al., 2006; Kabouridis et al., 1997; Koegl et al., 1994; Kosugi et al., 2001; van't Hof and Resh, 1999; Tewari et al., 2021; Wolven et al., 1997). These findings imply that the TCR signal transduction could be modulated by the enzymes catalyzing protein S-acylation, known as the DHHC family of protein acyltransferases (Baekkeskov and Kanaani, 2009). However, the exact identity of protein acyltransferases involved in TCR signaling, their regulatory mechanisms and physiological significance remained largely unknown. In our previous study aimed at identification of the S-acylating enzyme for Lck, we found that protein acyltransferase DHHC21, which is expressed in EL4 lymphoma cell line, has substrate preferences for Src-family kinases Lck and Fyn, and PLC-γ1, all of which have been recently identified as being S-acylated (Fan et al., 2020). Identification of key TCR signaling proteins as DHHC21 substrates suggested that this enzyme could be an important part of the proximal TCR signaling cascade. In this study, to further explore the role of the DHHC21 in regulation of TCR-induced T cell activation, we took advantage of the Zdhhc21^{dep} mouse strain in which a single phenylalanine residue (F233) within the C-terminal tail of DHHC21 is deleted (Mill et al., 2009).

We identified F233 as the first phenylalanine within a classical 1-14 Ca^{2+}/calmodulin-binding motif and found that deletion of this residue disrupts Ca^{2+}-dependent interaction between calmodulin and DHHC21. Given the well-known role of calmodulin in mediation of intracellular Ca^{2+} signals, this finding suggests that enzymatic activity of DHHC21 can be modulated by the cytoplasmic Ca^{2+} influx triggered upon TCR engagement. Indeed, in our previous study we have determined that S-acylation of DHHC21 substrate Lck was dependent on PLC-γ1-mediated Ca^{2+} release from the ER stores and that elimination of the Ca^{2+} signal prevented agonist-induced changes in Lck S-acylation (Akimzhanov and Boehning, 2015). Consistent with these observations, we found that disruption of the Ca^{2+}/calmodulin-binding motif of DHHC21 did not affect the basal S-acylation levels, but abrogated TCR-induced increase in S-acylation of DHHC21 protein targets. While more detailed studies are required to fully elucidate the mechanism of DHHC21 regulation, our findings indicate that, similar to what is found for other components of the TCR pathway, increases in enzymatic activity of DHHC21 can be rapidly triggered by the TCR-induced cytoplasmic Ca^{2+} influx.

Extremely rapid (within minutes) increase of protein S-acylation in response to agonist stimulation has been recently observed in several studies (Akimzhanov and Boehning, 2015; Chen et al., 2020; Fan et al., 2020; Tewari et al., 2021). However, the physiological meaning of these changes remained unclear since

Journal of Cell Science (2022) 135, jcs258186. doi:10.1242/jcs.258186

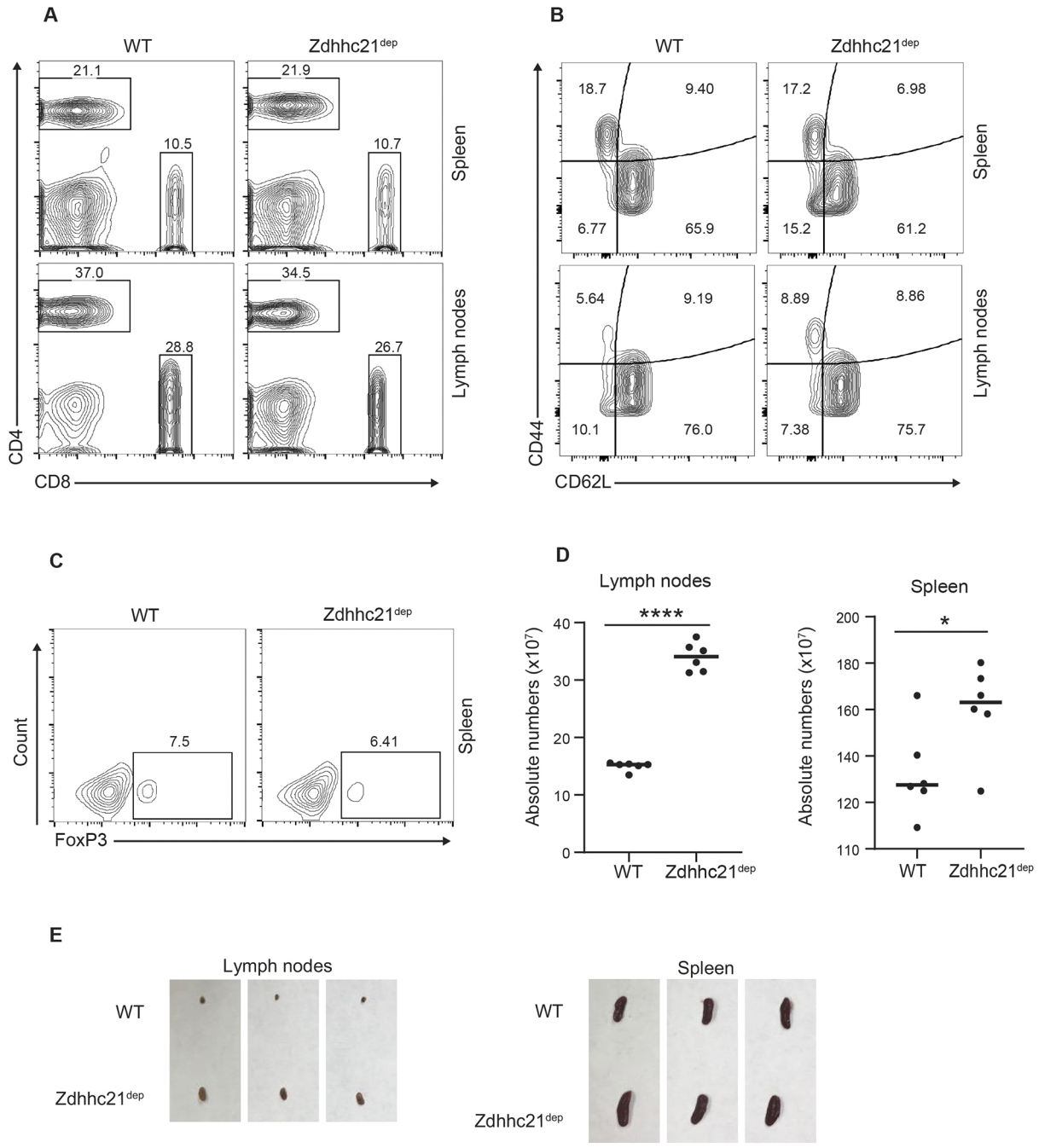

Fig. 6. T cell development in peripheral lymphoid organs of Zdhhc21^{dep} mice. (A) Flow cytometry analysis of cells isolated from spleen and lymph nodes of WT and Zdhhc21^{dep} mice. Plots of CD4$^+$ and CD8$^+$ cells are gated on CD3$^+$ cells. (B) Flow cytometry analysis of naïve (CD44^{lo}CD62L^{hi}) and effector memory (CD44^{hi}CD62L^{lo}) CD4$^+$ T cells isolated from spleen and lymph nodes of WT and Zdhhc21^{dep} mice. (C) Flow cytometry analysis of Treg cells isolated from spleens of WT and Zdhhc21^{dep} mice. Plots of FoxP3$^+$ cells are gated on CD4$^+$ cells. Values are percentages for each section. (D) The absolute numbers of thymocytes from WT and Zdhhc21^{dep} mice. Cell numbers were calculated based on the relative percentages determined by flow cytometry analysis and total cell numbers from thymus. ns, not significant, P>0.05 (two-tailed, unpaired Student's t-test). (E) Peripheral lymphoid organs in WT and Zdhhc21^{dep} mice. The fields of view shown are 2×4 cm (lymph nodes) and 4×8 cm (spleen).

conventional approaches to study the role of protein S-acylation rely on complete elimination of this modification through site-directed mutagenesis or pharmacological treatment. Our data suggests that the ΔF233 DHHC21 mutant preserves its basal enzymatic activity but is unable to respond to the TCR treatment by increasing S-acylation of its targets. Thus, the nature of the ΔF233 mutation provided us with a unique opportunity to examine the function of stimulus-dependent changes in S-acylation separately from the effects of S-acylation itself. We found that despite no detectable difference in basal protein S-acylation between WT and ΔF233 DHHC21 mice, CD4$^+$ T cells isolated from Zdhhc21^{dep} strain failed to respond to TCR stimulation, as evidenced by diminished activation of the proximal TCR pathway components, suppressed Ca^{2+} release and significantly reduced upregulation of major T cell activation markers. The fast kinetics of stimulus-induced protein S-acylation and its dramatic effect on T cell activation agree with a

Journal of Cell Science (2022) 135, jcs258186. doi:10.1242/jcs.258186

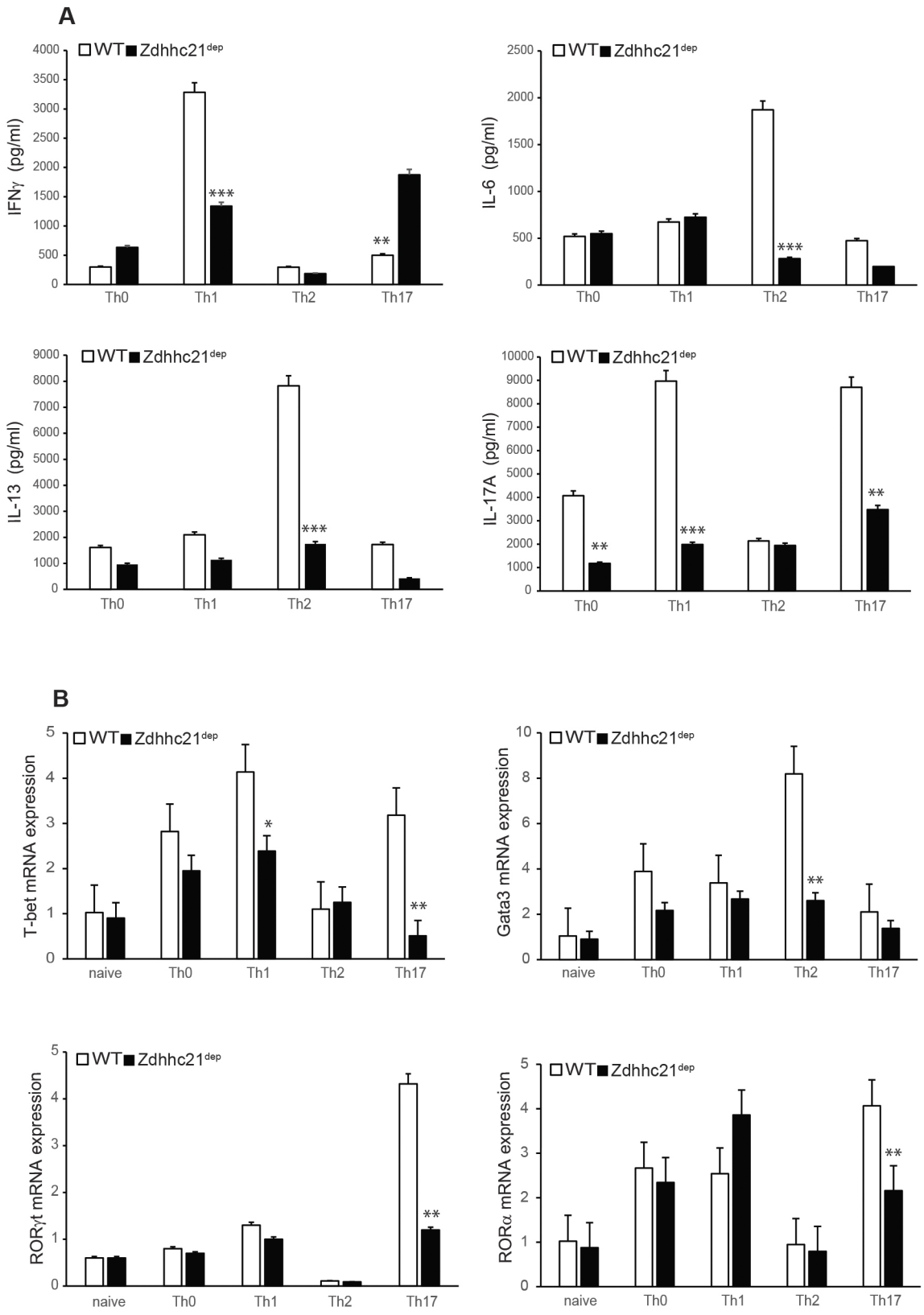

Fig. 7. DHHC21 regulates CD4⁺ T activation and differentiation. Naïve CD4⁺ T cells from WT or Zdhhc21^{dep} mice were stimulated with plate-bound anti-CD3–CD28 antibodies and incubated under neutral (Th0) or polarizing (Th1, Th2 and Th17) conditions for 5 days, then CD4⁺ T cells were re-stimulated with plate-bound anti-CD3 antibodies for 6 h. (A) Effector cytokine production measured by ELISA. The graph shows mean±s.d. values from at least three independent experiments. (B) mRNA expression of Th lineage-specific transcription factors determined by qRT-PCR normalized to 18S RNA. The graph shows mean±s.d., n=4, *P<0.05; **P<0.01; ***P<0.001 (two-tailed, unpaired Student's t-test).

Journal of Cell Science (2022) 135, jcs258186. doi:10.1242/jcs.258186

model in which DHHC21 is an integral part of the proximal TCR signaling machinery mediating the antigen signal transduction through rapid S-acylation of signaling proteins.

Initial T cell responses determine the long-term outcomes of TCR stimulation, such as development of immature T cells in the thymus and differentiation of naïve T cells in the peripheral lymphoid organs. We found that expression of ΔF233 DHHC21 had no apparent effect on populations of DN, DP and SP thymocytes suggesting that either DHHC21 is dispensable for T cell development or the reduced functionality of the ΔF233 mutant was sufficient to support DN-to-DP and DP-to-SP transitions during T cell maturation. However, we found that the inability of ΔF233 DHHC21 to respond to the TCR-induced Ca^{2+} signals significantly impaired differentiation of naïve $CD4^+$ T cells into Th1, Th2 and Th17 effector lineages. Furthermore, we noted that expression of the functionally deficient DHHC21 also resulted in increased size of spleen and lymph nodes accompanied by corresponding increase in absolute cell numbers. Although the underlying mechanism is unclear, it has been demonstrated previously that at least two of DHHC21 protein targets, PLC-γ1 and Lck, are critically involved in regulation of the Fas-mediated apoptosis and activation-induced T cell death (Akimzhanov et al., 2010; Wozniak et al., 2006; Yu et al., 2004). Therefore, it is possible that DHHC21 can play dual roles in regulating both TCR and Fas receptor signaling pathways and that the ΔF233 mutation of the DHHC21 regulatory domain makes T cells less susceptible to apoptosis in response to the Fas ligand in peripheral lymphoid organs, thus leading to increase in cell numbers. Overall, these findings suggest that DHHC21 plays a prominent role in peripheral immune responses and warrant further studies to investigate a potential role of DHHC21 in adaptive immunity and pathogenesis of the autoimmune diseases.

In summary, our study identifies protein acyltransferase DHHC21 as an essential component of the canonical TCR signaling pathway and demonstrates that this enzyme promotes early signal transduction by mediating rapid TCR-induced S-acylation of its protein targets. Our findings imply that protein acyltransferases, similar to other classes of regulatory enzymes, can play a vital function in regulation of T cell-mediated immunity and thus serve as potential drug targets in diseases associated with altered immune system homeostasis.

MATERIALS AND METHODS

Antibodies and reagents

Antibodies against the following proteins were purchased from Cell Signaling: Lck (Cat. 2787), p-Src (Cat. 2101), LAT (Cat. 45533), Fyn (Cat. 4023), p-Tyr-100 (Cat. 9411), p-PLC-γ1 (Cat. 8713), PLC-γ1 (Cat. 2824), p-ZAP-70 (Cat. 2717), ZAP-70 (Cat. 3165), p-Erk1/2 (Cat. 4370), ERK1/2 (Cat. 4376), JNK (Cat. 4668) and p-JNK (Cat. 9252). Anti-DHHC21 antibody was made in our laboratory (Fan et al., 2020). The following reagents were purchased from Sigma-Aldrich: Protein A Sepharose (Cat. p6649), hydroxylamine (Cat. 55459), S-methyl methanethiosulfonate (MMTS) (Cat. 208795), n-dodecyl β-D-maltoside (DDM) (Cat. D4641), thiopropyl-Sepharose 6B (Cat. T8387), poly-L-lysine (Cat. P8920), Phosphatase Inhibitor Cocktail 2 (Cat. P5726) and Complete Protease Inhibitor Cocktail tablets (Cat. 11836170001). ML211 (Cat. 17630) was purchased from Cayman. Cell-stimulating monoclonal antibodies (mAbs) were bought from BD Biosciences, San Diego, CA (anti-CD28), purified from a specific hybridoma (anti-CD3).

Mice

$Zdhhc21^{dep}$ mice were bred in our facility under specific pathogen-free conditions in accordance with the recommendations in the Guide for the Care and Use of Laboratory Animals of the National Institutes of Health. The animals were handled according to the animal care protocol (AWC 18-0131) approved by the Animal Welfare Committee (AWC), the Institutional Animal Care and Use Committee (IACUC) for the University of Texas Health Science Center at Houston (UTHealth). Mice used for experiments were males and females at 6–8 weeks old.

Western blotting

For protein immunoblotting, after the indicated stimulation, cells were washed twice with cold phosphate-buffered saline (PBS) and then lysed in 1% DDM lysis buffer [1% DDM in Dulbecco's phosphate-buffered saline (DPBS), 10 µM ML211, Phosphatase Inhibitor Cocktail 2 (1:100), Protease Inhibitor Cocktail (1×) and PMSF (10 mM)]. Protein concentration was determined by performing a Bio-Rad Bradford protein assay, and equal amounts of protein were loaded for immunoblot analysis. Lysates (30 µg protein) were separated by the SDS-PAGE, and then transferred to NC membranes (Bio-Rad). Membranes were blocked in 5% bovine serum albumin (BSA) in PBS-T (0.1% Tween-20 in PBS buffer) for 1 h at room temperature, and then incubated with the indicated primary antibodies at 1:1000 dilution overnight at 4°C. The membranes were then incubated with anti-mouse or anti-rabbit IgG conjugated to horseradish peroxidase at room temperature for 1 h. After three washes in PBS-T, membranes were imaged using the LI-COR Odyssey Scanner (LI-COR Biosciences; Lincoln, NE). Brightness and contrast were adjusted in the linear range using the Image Studio software (LI-COR).

Acyl-resin assisted capture assay

Protein S-acylation status was assessed by means of an acyl-RAC assay as described previously (Tewari et al., 2020). Cells were lysed in 1% DDM lysis buffer (as above). Post-nuclear cell lysate was subjected to chloroform-methanol precipitation and the protein pellet was resuspended in 400 µl of blocking buffer [0.2% (v/v) MMTS, 5 mM EDTA and 100 mM HEPES pH 7.4] and incubated for 15 min at 42°C. MMTS was removed by three rounds of chloroform-methanol precipitation and protein pellets were dissolved in 2SB buffer (2% SDS; 5 mM EDTA; 100 mM HEPES; pH 7.4). A tenth of each sample was retained as input control. For thioester bond cleavage and capture of free thiol groups, freshly prepared solution of neutral 2 M hydroxylamine solution (pH 7.0-7.5, final concentration 400 mM) was added together with thiopropyl Sepharose to each experimental sample. In negative control samples, the same concentration of sodium chloride was used instead of hydroxylamine. After 1 h incubation, beads were collected, and the proteins were eluted by incubation in SDS sample buffer supplemented with 5 mM DTT and analyzed by western blotting.

Immunoprecipitation

Cells were lysed in 1% DDM lysis buffer (as above). Then, 500 µg of lysate was used for each immunoprecipitation. A tenth of each sample was retained as input control. For immunoprecipitation, lysates were incubated overnight at 4°C with 1 µg of antibody against the protein of interest. This was followed by incubation with Protein A agarose beads for 4 h at 4°C. Immunoprecipitated proteins were eluted off beads by incubation with 1× Laemmli SDS sample buffer supplemented with 5 mM DTT for 15 min at 80°C with shaking. Eluted proteins were then analyzed by immunoblotting.

Quantitative real-time PCR

Total RNA was prepared from T cells using TriZol reagent (Invitrogen). cDNA was synthesized using Superscript reverse transcriptase and oligo(dT) primers (Invitrogen) and gene expression was examined with a Bio-Rad iCycler Optical System using iQ™ SYBR green real-time PCR kit (Bio-Rad Laboratories, Inc.). The data were normalized to 18S. Primers were: DHHC21, F, 5′-GGCTCTTTCTGCAGTTGTGT-3′, R, 5′-GGCCGCGATATTTCTTCACA-3′; T-bet, F, 5′-TGCGCCAGGAAGTTTCATTT-3′, R, 5′-GGGCTGGTACTTGTGGAGAGACT-3′; Gata3, F, 5′-GCAGCCTGCTGGGAGGAT-3′; R, 5′-TAGAGGTTGCCCCGCAGTT-3′; RORγτ, F, 5′-AGCATCTATAGCACTGACGG-3′, R, 5′-CAGAAACTGGGAATGCAGTG-3′; RORα, F, 5′-TCTCCCTGCGCTCTCCGCAC-3′, R, 5′-TCCACAGATCTTGCATGGA-3′.

In vitro differentiation and activation of naïve CD4$^+$ T cells

Naïve T cell differentiation was performed as described previously (Fan et al., 2020). Naïve CD4+ T cells were isolated from murine spleens and lymph nodes using naïve CD4$^+$ T cell purification kit (Miltenyi Biotech, Cat. 130-104-453) according to the manufacturer's instruction. Isolated T cells were activated with anti-CD3 and anti-CD28 (BD Pharmingen, 2 µg/ml) under Th0 (hIL-2, Peprotech, 50 U/ml), Th1 (anti-IL-4, Bioexcel, 10 µg/ml; IL-12, Peprotech, 10 ng/ml; hIL-2, 50 U/ml), Th2 (anti-IFN-γ, Bioexcel, 10 µg/ml; IL-4, Peprotech, 10 ng/ml; hIL-2, 50 U/ml) and Th17 (anti-IFN-γ, 10 µg/ml; anti-IL-4, 10 µg/ml; IL-6, Peprotech, 20 ng/ml; TGF-β, Peprotech, 2 ng/ml) polarizing conditions for 4 days. Then, cells were re-stimulated with anti-CD3–CD28 for 4 h. Supernatant was collected to assess cytokine production by ELISA (R&D Systems) and differentiated cells were used for mRNA expression analysis.

For T cell activation, WT or DHHC21^{dep} T cells were purified using CD4$^+$ T cell isolation kit (Miltenyi Biotech, Cat. 130-104-453) and activated with plate-bound anti-CD3 and/or anti-CD28 (eBioscience). IL-2 production was determined 24 h after T-cell activation by ELISA according to manufacturer's instructions (R&D Systems). CD69 production was analyzed by flow cytometry after 2 days of anti-CD3 and/or anti-CD28 stimulation.

Flow cytometry

Splenocytes were harvested and single-cell suspensions were prepared in PBS in 5% fetal calf serum (FCS) buffer. Cells were kept on ice during all the procedures. For the extracellular markers, cells were stained with appropriate surface antigens. The following antibodies were obtained from BD eBioscience, or Invitrogen and were as follows: PerCP-Cy5.5-conjugated anti-CD3 (clone SK7, 1:20 dilution), CD4 PE (clone GK1.5, 1:200), CD8 FITC (clone 5H10-1, 1:800), CD62L FITC (clone MEL-14, 1:800 dilution), CD44 APC (clone IM7, 1:500 dilution), CD69 PE (clone H1.2F3, 1:100 dilution), CD25 FITC (clone 3c7, 1:100 dilution), FoxP3 APC (clone FJK-16S, 1:200 dilution). Live/dead assays were performed using the Aqua Dead Cell Stain Kit (Thermo Fisher Scientific, Cat. L34957). Gating was determined using the Fluorescence minus one approach. Detection of cell surface markers was conducted using a Beckman-Coulter Gallios Flow Cytometer (BD Biosciences, San Jose, CA, USA) and data were analyzed by Kaluza Analysis Software, BD FACs Canto and FlowJo v. 10.6.2.

Fura-2 Ca^{2+} imaging

Cells were loaded with Fura-2 AM as described previously (Akimzhanov et al., 2010; Wozniak et al., 2006) and placed in an imaging chamber with a glass bottom pre-coated with poly-L-lysine. Images were taken on a Nikon TiS inverted microscope (Tokyo, Japan) with a 40× oil immersion objective, and images were taken every 3 s with a Photometrics Evolve electron-multiplying charged-coupled device camera (Tucson, AZ). Cells were pre-treated with αCD3 antibody and secondary IgG antibody was added after baseline recording to initiate TCR signaling.

Acknowledgements

We thank Ethan Marin (Yale School of Medicine) for providing us with the Zdhhc21^{dep} mouse strain.

Competing interests

The authors declare no competing or financial interests.

Author contributions

Conceptualization: S.B., D.B., A.M.A.; Methodology: S.B., Y.F., S.J.W., R.T., J.K., T.M., A.M.A.; Software: S.B., A.M.A.; Validation: S.B., Y.F., R.T., A.M.A.; Formal analysis: S.B., Y.F., S.J.W., R.T., J.K., A.M.A.; Investigation: S.B., D.B., A.M.A.; Resources: S.B., D.B., A.M.A.; Data curation: S.B., Y.F., S.J.W., T.M., A.M.A.; Writing - original draft: S.B., A.M.A.; Writing - review & editing: S.B., A.M.A.; Visualization: S.B., A.M.A.; Supervision: D.B., A.M.A.; Project administration: A.M.A.; Funding acquisition: D.B., A.M.A.

Funding

This work was supported by startup funding from McGovern Medical School at University of Texas Health Science Center (to A.M.A.) and National Institute of General Medical Sciences grants R01GM115446 (to A.M.A.) and R01GM081685 (to D.B.). Deposited in PMC for release after 12 months.

References

Akimzhanov, A. M. and Boehning, D. (2015). Rapid and transient palmitoylation of the tyrosine kinase Lck mediates Fas signaling. *Proc. Natl. Acad. Sci. USA* **112**, 11876-11880. doi:10.1073/pnas.1509929112

Akimzhanov, A. M., Wang, X., Sun, J. and Boehning, D. (2010). T-cell receptor complex is essential for Fas signal transduction. *Proc. Natl. Acad. Sci. USA* **107**, 15105-15110. doi:10.1073/pnas.1005419107

Au-Yeung, B. B., Shah, N. H., Shen, L. and Weiss, A. (2018). ZAP-70 in signaling, biology, and disease. *Annu. Rev. Immunol.* **36**. 127-156. doi:10.1146/annurev-immunol-042617-053335

Baekkeskov, S. and Kanaani, J. (2009). Palmitoylation cycles and regulation of protein function (Review). *Mol. Membr. Biol.* **26**, 42-54. doi:10.1080/09687680802680108

Beard, R. S., Yang, X., Meegan, J. E., Overstreet, J. W., Yang, C. G. Y., Elliott, J. A., Reynolds, J. J., Cha, B. J., Pivetti, C. D., Mitchell, D. A. et al. (2016). Palmitoyl acyltransferase DHHC21 mediates endothelial dysfunction in systemic inflammatory response syndrome. *Nat. Commun.* **7**, 12823. doi:10.1038/ncomms12823

Brownlie, R. J. and Zamoyska, R. (2013). T cell receptor signalling networks: branched, diversified and bounded. *Nat. Rev. Immunol.* **13**, 257-269. doi:10.1038/nri3403

Chen, J. J., Marsden, A. N., Scott, C. A., Akimzhanov, A. M. and Boehning, D. (2020). DHHC5 Mediates β-Adrenergic signaling in Cardiomyocytes by targeting Gα proteins. *Biophys. J.* **118**, 826-835. doi:10.1016/j.bpj.2019.08.018

Fan, Y., Shayahati, B., Tewari, R., Boehning, D. and Akimzhanov, A. M. (2020). Regulation of T cell receptor signaling by protein acyltransferase DHHC21. *Mol. Biol. Rep.* **47**, 6471-6478. doi:10.1007/s11033-020-05691-1

Hundt, M., Tabata, H., Jeon, M.-S., Hayashi, K., Tanaka, Y., Krishna, R., De Giorgio, L. , Liu, Y.-C., Fukata, M. and Altman, A. (2006). Impaired activation and localization of LAT in Anergic T cells as a consequence of a selective palmitoylation defect. *Immunity* **24**, 513-522. doi:10.1016/j.immuni.2006.03.011

Kabouridis, P. S., Magee, A. I. and Ley, S. C. (1997). S-acylation of LCK protein tyrosine kinase is essential for its signalling function in T lymphocytes. *EMBO J.* **16**, 4983-4998. doi:10.1093/emboj/16.16.4983

Katz, Z. B., Novotná, L., Blount, A. and Lillemeier, B. F. (2017). A cycle of Zap70 kinase activation and release from the TCR amplifies and disperses antigenic stimuli. *Nat. Immunol.* **18**, 86-95. doi:10.1038/ni.3631

Koegl, M., Zlatkine, P., Ley, S. C., Courtneidge, S. A. and Mageet, A. I. (1994). Palmitoylation of multiple Src-family kinases at a homologous N-terminal motif. *Proteins* **303**, 749-753. doi:10.1042/bj3030749

Kosugi, A., Hayashi, F., Liddicoat, D. R., Yasuda, K., Saitoh, S.-I. and Hamaoka, T. (2001). A pivotal role of cysteine 3 of Lck tyrosine kinase for localization to glycolipid-enriched microdomains and T cell activation. *Immunol. Lett.* **76**, 133-138. doi:10.1016/S0165-2478(01)00174-2

Lewis, R. S. (2001). Calcium signaling mechanisms in T lymphocytes. *Annu. Rev. Immunol.* **19**, 497-521. doi:10.1146/annurev.immunol.19.1.497

Marin, E. P., Jozsef, L., Di Lorenzo, A., Held, K. F., Luciano, A. K., Melendez, J., Milstone, L. M., Velazquez, H. and Sessa, W. C. (2016). The protein Acyl Transferase ZDHHC21 modulates α1 adrenergic receptor function and regulates hemodynamics. *Arterioscler. Thromb. Vasc. Biol.* **36**, 370-379. doi:10.1161/ATVBAHA.115.306942

Mayer, T. C., Kleiman, N. J. and Green, M. C. (1976). Depilated (dep), a mutant gene that affects the coat of the mouse and acts in the epidermis. *Genetics* **84**, 59-65.

Michelangeli, F. and East, J. M. (2011). A diversity of SERCA Ca2+ pump inhibitors. *Biochem. Soc. Trans.* **39**, 789-797. doi:10.1042/BST0390789

Mill, P., Lee, A. W. S., Fukata, Y., Tsutsumi, R., Fukata, M., Keighren, M., Porter, R. M., McKie, L., Smyth, I. and Jackson, I. J. (2009). Palmitoylation regulates epidermal homeostasis and hair follicle differentiation. *PLoS Genet.* **5**, e1000748. doi:10.1371/journal.pgen.1000748

Oh-hora, M. (2009). Calcium signaling in the development and function of T-lineage cells. *Immunol. Rev.* **231**, 210-224. doi:10.1111/j.1600-065X.2009.00819.x

Palacios, E. H. and Weiss, A. (2004). Function of the Src-family kinases, Lck and Fyn, in T-cell development and activation. *Oncogene* **23**, 7990-8000. doi:10.1038/sj.onc.1208074

Ren, W., Jhala, U. S. and Du, K. (2013). Proteomic analysis of protein palmitoylation in adipocytes. *Adipocyte* **2**, 17-27. doi:10.4161/adip.22117

Resh, M. D. (2016). Fatty acylation of proteins: the long and the short of it. *Prog. Lipid Res.* **63**, 120-131. doi:10.1016/j.plipres.2016.05.002

Salmond, R. J., Filby, A., Qureshi, I., Caserta, S. and Zamoyska, R. (2009). T-cell receptor proximal signaling via the Src-family kinases, Lck and Fyn, influences T-cell activation, differentiation, and tolerance. *Immunol. Rev.* **228**, 9-22. doi:10.1111/j.1600-065X.2008.00745.x

Smith-Garvin, J. E., Koretzky, G. A. and Jordan, M. S. (2009). T cell activation. *Annu. Rev. Immunol.* **27**, 591-619. doi:10.1146/annurev.immunol.021908.132706

Stathopulos, P. B., Zheng, L., Li, G.-Y., Plevin, M. J. and Ikura, M. (2008). Structural and mechanistic insights into STIM1-mediated initiation of store-operated calcium entry. *Cell* **135**, 110-122. doi:10.1016/j.cell.2008.08.006

Su, X., Ditlev, J. A., Hui, E., Xing, W., Banjade, S., Okrut, J., King, D. S., Taunton, J., Rosen, M. K. and Vale, R. D. (2016). Phase separation of signaling molecules promotes T cell receptor signal transduction. *Science* **352**, 595-599. doi:10.1126/science.aad9964

Tewari, R., West, S. J., Shayahati, B. and Akimzhanov, A. M. (2020). Detection of protein S-Acylation using Acyl-resin assisted capture. *J. Vis. Exp.* **158**, e61016.doi:10.3791/61016

Tewari, R., Shayahati, B., Fan, Y. and Akimzhanov, A. M. (2021). T cell receptor–dependent S-acylation of ZAP-70 controls activation of T cells. *J. Biol. Chem.* **296**, 100311. doi:10.1016/j.jbc.2021.100311

van't Hof, W. and Resh, M. D. (1999). Dual Fatty Acylation of p59 ^{Fyn} is required for association with the T cell receptor ζ Chain through phosphotyrosine–Src homology domain-2 interactions. *J. Cell Biol.* **145**, 377-389. doi:10.1083/jcb.145.2.377

Wolven, A., Okamura, H., Rosenblatt, Y. and Resh, M. D. (1997). Palmitoylation of p59fyn is reversible and sufficient for plasma membrane association. *Mol. Biol. Cell* **8**, 1159-1173. doi:10.1091/mbc.8.6.1159

Wozniak, A. L., Wang, X., Stieren, E. S., Scarbrough, S. G., Elferink, C. J. and Boehning, D. (2006). Requirement of biphasic calcium release from the endoplasmic reticulum for Fas-mediated apoptosis. *J. Cell Biol.* **175**, 709-714. doi:10.1083/jcb.200608035

Yu, X.-Z., Levin, S. D., Madrenas, J. and Anasetti, C. (2004). Lck is required for activation-induced T cell death after TCR ligation with partial agonists. *J. Immunol.* **172**, 1437-1443. doi:10.4049/jimmunol.172.3.1437

Zhou, L., Chong, M. M. W. and Littman, D. R. (2009). Plasticity of CD4+ T cell lineage differentiation. *Immunity* **30**, 646-655. doi:10.1016/j.immuni.2009.05.001

Fig. S1

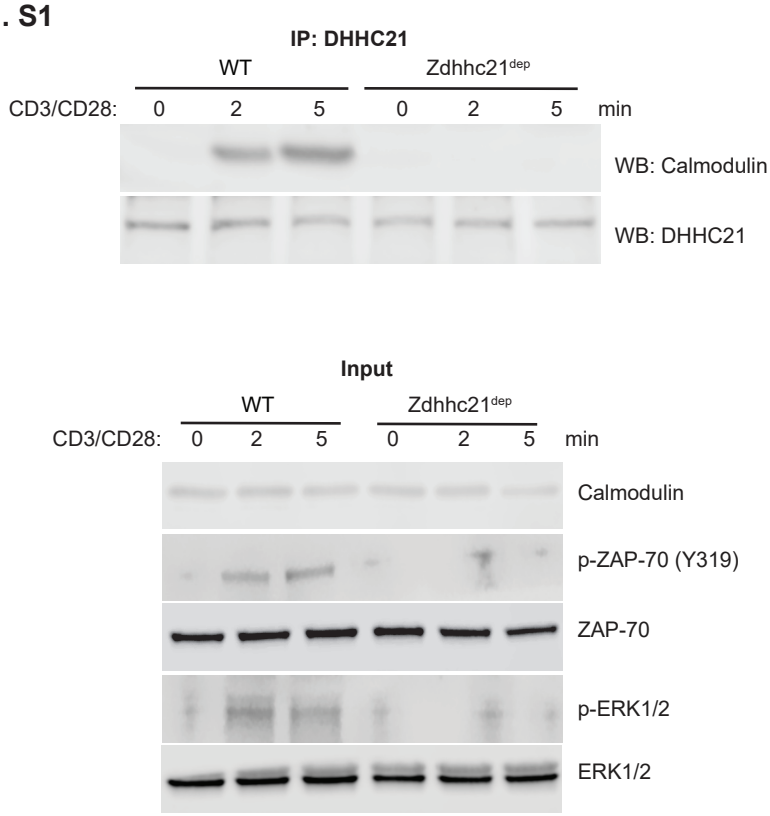

Fig. S1:TCR-dependent co-immunoprecipitation of DHHC21 and calmodulin. CD4⁺ T cells from WT or Zdhhc^{dep} mice were stimulated for indicated times with anti-CD3/CD28 antibody to evoke calcium release. DHHC21 was immunoprecipitated from the cell lysates and binding of calmodulin was detected by immunoblotting. Total lysates (20% load) are depicted as input. Phosphorylated ZAP-70 and ERK1/2 are shown to confirm CD4⁺ T cells' responses to TCR-stimulation.